SURFACE POWER DISTRIBUTION IN CROSS FIELD HEATING OF THIN NONMAGNETIC PLATES

K.V.Namjoshi and P.P.Biringer

Electrical Engineering Department,
University of Toronto, Toronto, Ontario,
M5S 1A4 Canada.

Abstract - **In this paper, the problem of non-uniformity of the induced surface power density in the workpieces of cross-field heating systems is analyzed. Assuming the workpiece to be very thin, the induced current density and the induced power density are obtained using a method based on circuit theory. Calculation of the total power agrees with the measured value. The results suggest that to obtain uniform current density, one may have to try different shapes for the exciting coils. Varying the distance between the coils or their lengths does not produce the desired effect.**

I. INTRODUCTION

In cross-field heating systems, which are used in the heat treatment of long thin plates, the exciting field is essentially perpendicular to the object or the workpiece to be heated[1]. In the past, cross-field systems have been analyzed using simple models[2-5]. In these systems, the distribution of the induced current or the power is of interest because it determines the distribution of the heat produced. This being a three dimensional problem, the exact solution needs large computer memory and is time consuming[6]. In this paper, we use a method based on circuit theory, which is a form of integral equations, to obtain the current density distribution. The workpiece is represented by an infinitesimally thin sheet. Results are presented for the induced current density for rectangular and oval shaped coils to bring out the effects of parameters such as the coil separation, coil length, polarity of the coil current and frequency. Single-sided air-cored systems with non-magnetic loads are considered.

II. METHOD

The schematic diagram of the arrangement studied is shown in Fig.1. It has two exciting coils and a thin workpiece at a distance l_g from the coils. d is the distance between the coils and l is the coil length. If d is small in comparison with coil dimensions, the field produced by the coils is mostly transverse to the workpiece. In thin workpieces, the thickness of the workpiece is much smaller than the other system dimensions and the skin depth of the workpiece. Therefore, the variation of the field variables along the thickness of the workpiece can be neglected and the problem can be analyzed as a surface power density problem by assuming the workpiece to be an infinitesimally thin sheet[7]. In the method

Manuscript received February 17, 1992.

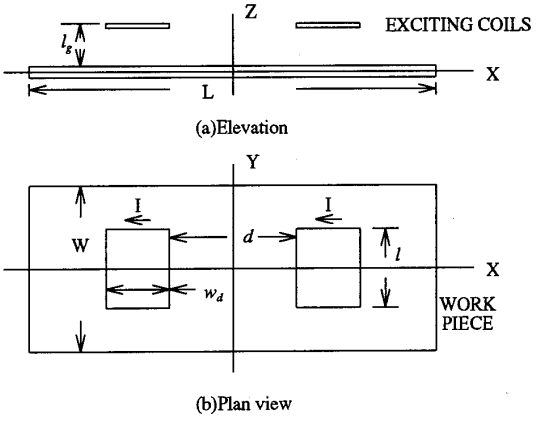

Figure 1: Schematic diagram of a single sided, air cored cross-field heating system showing the heater coils and the work piece. The coils carry current I in the same direction.

used the surface of the workpiece is divided into a square mesh(Fig.2).

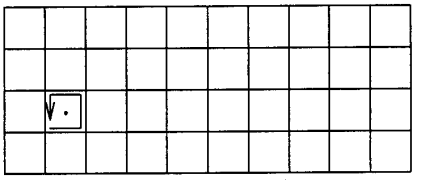

Figure 2: Division of the workpiece into a square mesh showing a mesh current.

The currents induced in the mesh are obtained by the solution of the following circuit equations which are derived from the integral forms of Faraday's and Ampere's laws[8]:

$$[D][I_M] = -k^2h^2[H_0] - k^2h^2[H_{ind}] \quad (1)$$

$$\text{and} \quad [H_{ind}] = [C][I_M]. \quad (2)$$

Here, $[I_M]$, $[H_0]$ and $[H_{ind}]$ are column vectors representing the mesh currents, the Z component of the incident magnetic field and the Z component of the induced magnetic field. [D] is the resistance matrix[9]. $k^2 = \sqrt{j\omega\mu_0\sigma}$, $\omega = 2\pi f$ the frequency, σ the conductivity and μ_0 the permeability of the free space. In computing matrix $[D]$, the resistance of individual cell side, R_S, is obtained by:

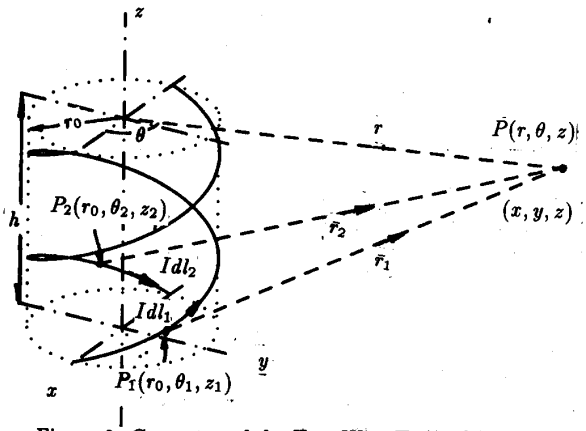

Figure 2: Geometry of the Two-Wire Twisted-Pair Transmission Line

where the symbol NP denotes the number of pitches. Meanwhile, $\bar{r}_1$ denotes the space vector from the source point, P_1, on conductor #1 to the observation point, P, and $\bar{r}_2$ denotes the space vector from the source point, P_2, on conductor #2 to point, P. Here, $\bar{r}_1$ and $\bar{r}_2$ are the space vectors from the source points, P_1 and P_2, on conductor #1 and conductor #2 to the observation point, P, respectively, which are given as follows:

$$\bar{r}_1 = (x - r_0\cos\theta_1)\hat{a}_x + (y - r_0\sin\theta_1)\hat{a}_y + (z - \frac{h}{2\pi}\theta_1)\hat{a}_z \quad (4)$$

$$\bar{r}_2 = (x + r_0\cos\theta_1)\hat{a}_x + (y - r_0\sin\theta_1)\hat{a}_y + (z - \frac{h}{2\pi}\theta_1)\hat{a}_z \quad (5)$$

Using vector operation rules, one may obtain the following:

$$d\bar{l}_1 \times \bar{r}_1 = \begin{vmatrix} \hat{a}_x & \hat{a}_y & \hat{a}_z \\ -r_0\sin\theta_1 d\theta_1 & r_0\cos\theta_1 d\theta_1 & \frac{h}{2\pi}d\theta_1 \\ x - r_0\cos\theta_1 & y - r_0\sin\theta_1 & z - \frac{h}{2\pi}\theta_1 \end{vmatrix} \quad (6)$$

and,

$$-d\bar{l}_2 \times \bar{r}_2 = \begin{vmatrix} \hat{a}_x & \hat{a}_y & \hat{a}_z \\ -r_0\sin\theta_1 d\theta_1 & r_0\cos\theta_1 d\theta_1 & -\frac{h}{2\pi}d\theta_1 \\ x + r_0\cos\theta_1 & y + r_0\sin\theta_1 & z - \frac{h}{2\pi}\theta_1 \end{vmatrix} \quad (7)$$

Substituting (6) and (7) into (3), one can obtain the formulation of the flux density as follows:

$$\bar{B}(x,y,z) = \frac{\mu_0 I}{4\pi}\sum_{i=-NP/2}^{NP/2-1}\int_{2\pi i}^{2\pi(i+1)} \left(\frac{1}{r_1^3}\begin{bmatrix} r_0\cos\theta_1(z - \frac{h}{2\pi}\theta_1) - (y - r_0\sin\theta_1)\frac{h}{2\pi} \\ (x - r_0\cos\theta_1)\frac{h}{2\pi} + r_0\sin\theta_1(z - \frac{h}{2\pi}\theta_1) \\ -r_0\sin\theta_1(y - r_0\sin\theta_1) - r_0\cos\theta_1(x - r_0\cos\theta_1) \end{bmatrix} + \frac{1}{r_2^3}\begin{bmatrix} r_0\cos\theta_1(z - \frac{h}{2\pi}\theta_1) + (y + r_0\sin\theta_1)\frac{h}{2\pi} \\ -(x + r_0\cos\theta_1)\frac{h}{2\pi} + r_0\sin\theta_1(z - \frac{h}{2\pi}\theta_1) \\ -r_0\sin\theta_1(y + r_0\sin\theta_1) - r_0\cos\theta_1(x + r_0\cos\theta_1) \end{bmatrix} \right) d\theta_1 \quad (8)$$

Those integral formulations were computed with the help of the Gaussian numerical integral method [2], which is readily suited for digital computation. Details are given in reference [4].

III. RESULTS

The resulting magnetic flux density, $\bar{B}$, specifically the B_x and B_y components, can be computed at any cross-section as shown in Figure(1) for a cross-section perpendicular to the $z-$axis. Here, this calculation was performed at locations along the three concentric circles shown by the dotted lines in Figure(3). Also, depicted in Figure (3) are the x and y components of the resulting $\bar{B}$ field. Meanwhile, the $z-$components of the resulting $\bar{B}$ field are shown in Figure (4).

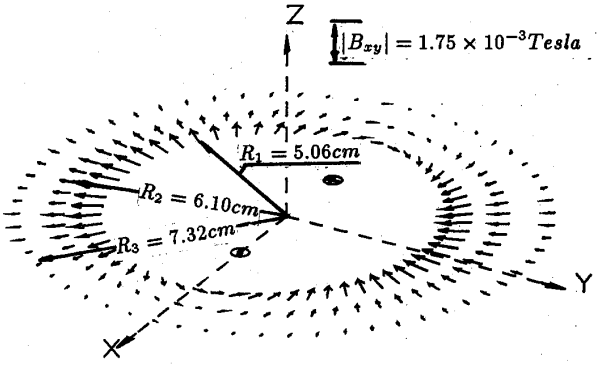

Figure 3: Flux Density Components B_x and B_y for the Twisted-Pair, h=12.7cm, for a Current $I = 500A$

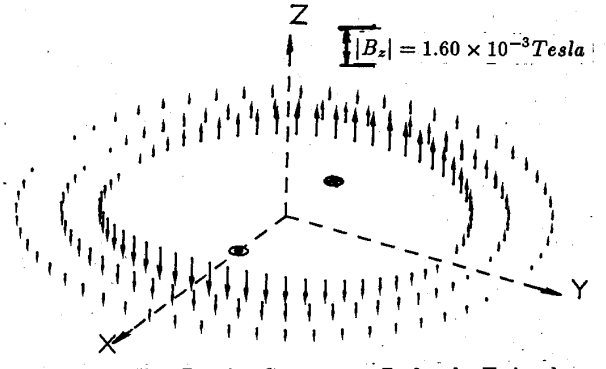

Figure 4: Flux Density Component B_z for the Twisted-Pair, h=12.7cm, for a Current $I = 500A$

The resulting $\bar{B}$ field, Figures (3) and (4), at various points along the three dotted circles is shown by the $\bar{B}$ vector arrow displays, whose directions indicate the orientation of the $\bar{B}$ field in the $x - y$ plane as well as the $z-$direction, and whose length is proportional to the magnitude of the resultant $\bar{B}$ field along the $x-y$ plane and the component along the

$z-$axis. These $\overline{B}$ field results shown in Figures (3) and (4) are for the twisted-pair case with a pitch, $h = 12.7cm(= 5in.)$, and at a plane with $z = 0$.

The effects of the choice of the pitch, h, defined in Figure(2), on the flux density components, B_x, B_y, and B_z, are documented in Figures(5) through (7) at the mid-plane point (z=0) for a transmission line of length $508m(= 20000in.)$. For all these cases, in Figure(2), r_0 is equal to $2.54cm(= 1in.)$. The above is given for a $500A$ DC current flowing in opposite direction in each conductor.

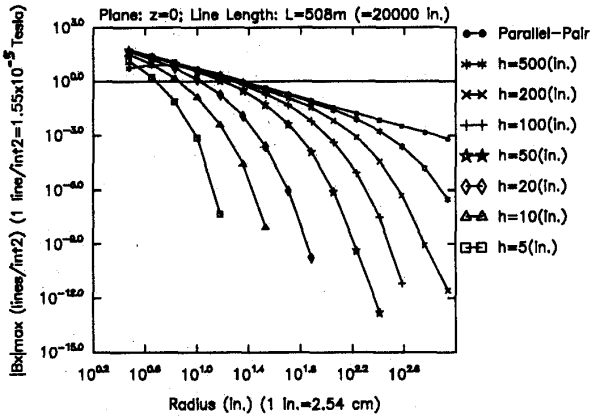

Figure 5: Magnitudes of Flux Density Component $|B_x|_{max}$ for Different Pitch lengths,for $I = 500A$

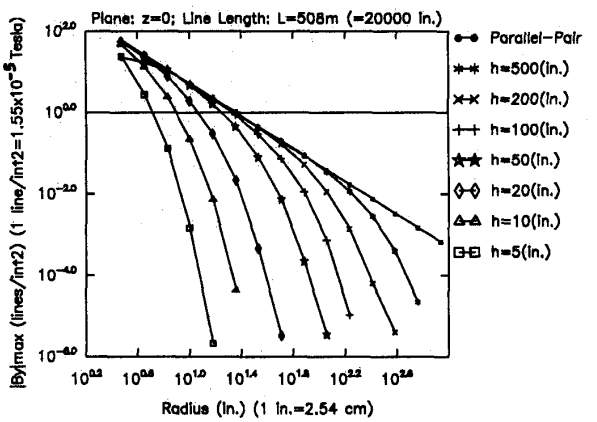

Figure 6: Magnitudes of Flux Density Component $|B_y|_{max}$ for Different Pitch lengths,for $I = 500A$

Figures (5) through (7) show the effects of varying the helical twist pitch on the $\overline{B}$ field resulting from a (508 m) fixed length transmission line. Notice that as the pitch approaches infinity the resulting magnetic field approaches the field pattern of a two-parallel-pair transmission line. There are no z-component $\overline{B}$ fields resulting from the parallel-pair case, while there are z-component $\overline{B}$ fields resulting from the twisted-pair case as shown in Figure(7). The results also reveal as expected, that shorter lengths of the helical pitch cause the

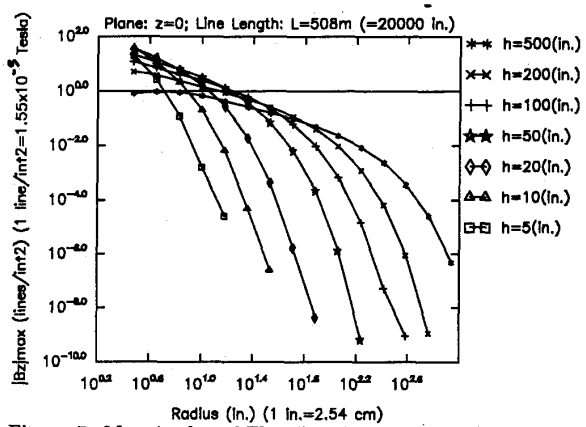

Figure 7: Magnitudes of Flux Density Component $|B_z|_{max}$ for Different Pitch lengths,for $I = 500A$

$\overline{B}$ fields outside the transmission line to decay more quickly in the radially outward direction. Thus shorter pitches lead to reduced magnitudes of background magnetic field, which is a desirable outcome from the SSF electromagnetic field compatibility point of view. Examination of Figures (5) through (7), leads one to conclude that at locations far away from the transmission line, the z-component of the fields, B_z, is of the same order of magnitude as that of the x, and y components, B_x and B_y.

IV. CONCLUSIONS

The results obtained from this analytical method show the 3D nature of the $\overline{B}$ field surrounding a two-wire twisted-pair transmission line in the static case. That is, the twisted-pair problem should be dealt with using 3D magnetic field computation methods if geometrically complicating surroundings such as shields and highly permeable materials are present. Therefore, some new methods are needed for studying shielding effects and defects surrounding those types of twisted-pair wires. The 3D nature of this field means that in future work one of the available options may be to use 3D finite element analysis in conjunction with ballooning techniques to evaluate the shielding problems and effects of a conducting plasma environment, when AC cases of interest in SSF power transmission lines are studied.

REFERENCES

[1] S. Ratnajeevan H. Hoole, *Computer-Aided Analysis and Design of Electromagnetic Devices*, New York, NY, Elsevier Science Publishing Co., Inc. 1989.

[2] W. Cheney, *Numerical Mathematics and Computing*, Pacific Grove, CA, Brooks /Cole Publishing Co. 1985.

[3] P. Moon, et al, *Foundations of Electrodynamics*, Cambridge, MA, Boston Technical Publishers, Inc. 1965.

[4] Z. Luo, "Electromagnetic Fields Surrounding Transmission Lines in Space Station Applications Using Finite Elements and Ballooning Methods for Simulation of Infinite Boundaries", *Master's Thesis*, Clarkson University, Potsdam, NY, 1991.